Published in final edited form as:
Nat Sustain. 2019 ; 2: 122–129. doi:10.1038/s41893-019-0220-7.

China and India lead in greening of the world through land-use management

Chi Chen[1], **Taejin Park**[1], **Xuhui Wang**[2], **Shilong Piao**[2], **Baodong Xu**[1,3], **Rajiv K. Chaturvedi**[4], **Richard Fuchs**[5], **Victor Brovkin**[6], **Philippe Ciais**[7], **Rasmus Fensholt**[8], **Hans Tømmervik**[9], **Govindasamy Bala**[10], **Zaichun Zhu**[11], **Ramakrishna R. Nemani**[12], and **Ranga B. Myneni**[1]

[1]Department of Earth and Environment, Boston University, Boston, MA 02215, USA

[2]Sino-French Institute for Earth System Science, College of Urban and Environmental Sciences, Peking University, Beijing 100871, China

[3]College of Resource and Environment, Huazhong Agricultural University, 1 Shizishan Street, Wuhan 430070, China

[4]Birla Institute of Technology and Science, Pilani, Goa 403726, India

[5]Institute of Meteorology and Climate Research – Atmospheric Environmental Research, Karlsruhe Institute of Technology, 82467 Garmisch-Partenkirchen, Germany

[6]Max-Planck-Institute for Meteorology, Bundesstrasse 53, 20146 Hamburg, Germany

[7]Laboratoire des Sciences du Climat et de l'Environnement/IPSL, CEA-CNRS-UVSQ, Université Paris Saclay, Gif-sur-Yvette, France

[8]Department of Geosciences and Natural Resource Management, University of Copenhagen, Copenhagen, Denmark

[9]Norwegian Institute for Nature Research, Fram Centre, 9296 Tromsø, Norway

[10]Center for Atmospheric and Oceanic Sciences, Indian Institute of Science, Bangalore, Karnataka 560012, India

[11]Shenzhen Key Laboratory of Circular Economy, Shenzhen Graduate School, Peking University, Shenzhen 518055, China

[12]NASA Ames Research Center, Moffett Field, CA 94035, USA

Correspondence and requests for materials should be addressed to C.C (chenchi@bu.edu).

Author Contributions C.C. carried out the analyses with contributions from T.P., X.W., B.X., R.K.C. and R.F. C.C. and R.M.B. wrote the article. All authors contributed ideas for analyses, comments and critiques on drafts.

Competing interests

The authors declare no competing financial interests.

Data availability.

The datasets generated during and/or analysed in this study are publicly available as referenced within the article. All data and scripts are available from the corresponding author on request.

Additional information

Supplementary information is available in the online version of the paper. Reprints and permissions information is available online at www.nature.com/reprints.

Abstract

Satellite data show increasing leaf area of vegetation due to direct (human land-use management) and indirect factors (climate change, CO_2 fertilization, nitrogen deposition, recovery from natural disturbances, etc.). Among these, climate change and CO_2 fertilization effect seem to be the dominant drivers. However, recent satellite data (2000–2017) reveal a greening pattern that is strikingly prominent in China and India, and overlapping with croplands world-wide. China alone accounts for 25% of the global net increase in leaf area with only 6.6% of global vegetated area. The greening in China is from forests (42%) and croplands (32%), but in India is mostly from croplands (82%) with minor contribution from forests (4.4%). China is engineering ambitious programs to conserve and expand forests with the goal of mitigating land degradation, air pollution and climate change. Food production in China and India has increased by over 35% since 2000 mostly due to increasing harvested area through multiple cropping facilitated by fertilizer use and surface/ground-water irrigation. Our results indicate that the direct factor is a key driver of the "Greening Earth", accounting for over a third, and likely more, of the observed net increase in green leaf area. They highlight the need for realistic representation of human land-use practices in Earth system models.

Green leaves of vegetation sustain life on Earth by synthesizing sugars from water and carbon dioxide (CO_2) using the energy of sunlight and cool the surface by transpiring large amounts of water during this process. Their abundance is measured as one-sided leaf area in broadleaf species and one-half the total needle surface area in coniferous species[1]. This varies seasonally between a maximum of 231×10^6 km^2 in July, when the Northern Hemisphere is at its greenest, and a minimum of 132×10^6 km^2 in January. The yearly average of 171×10^6 km^2 of leaf area displayed on 109×10^6 km^2 of vegetated area represents the annual average leaf area index (LAI) of the Earth (1.57). Greening (browning) is defined as a statistically significant increase (decrease) in annual-average green leaf area at a location over a period of several years. It could result from changes in average leaf size, leaf number per plant, plant density, species composition, duration of green-leaf presence due to changes in growing season and multiple cropping, etc.

Data from satellites, available since the early 1980s, indicate increasing greenness over the Earth's lands, from Svalbard to Australia and from Alaska to Chukotka[2–7]. The previously inferred dominant role of CO_2 fertilization effect[7–11], and of indirect drivers in general[2,7,12–17], in greening of the Earth raises the question – what is the role of human land-use in shaping the vegetation greenness patterns on global lands? It may be more important than currently thought, for the following reasons. First, the models used in previous attribution analyses have rudimentary representation of evolving complex patterns of land-use practices detailed below and elsewhere[18], thus downplaying the direct role of human hand in greening[19]. Second, the effects of higher CO_2 concentration on plant growth[20], outside of experimental situations, are poorly understood and consequently the models differ widely in their prognostications[21]. Third, deleterious effects of sensor calibration loss, satellite orbital drift, atmospheric contamination of vegetation signals and disjointed stitching of data from multiple sequential sensors are evident in the underlying satellite data[22] used in nearly all previous studies. Fourth, a recent study reveals that human land-use is the dominant factor behind changes in woody and herbaceous vegetation cover[23].

Now that better quality leaf area data are available from the Moderate Resolution Imaging spectroradiometer (MODIS) sensor observations[1,24–26] – Supplementary Table 1 lays out in detail the specifics of MODIS *vs.* AVHRR (Advanced Very High Resolution Radiometer) data – we aim here to assess the role of the direct driver, without recourse to models, by characterizing the greening patterns in ecosystems globally.

Results

The Earth is greening.

According to MODIS data, one-third of the global vegetated area is greening and 5% is browning. This translates to a net increase in leaf area of 2.3% per decade (Fig. 1 & Supplementary Table 2), which is equivalent to adding 5.4×10^6 km^2 of new leaf area over the 18-yr period of the record (2000 to 2017, Table 1). Two-thirds of this greening is from croplands and forests in about equal measure (Supplementary Table 3). The greening is prominently clustered in seven regions across six continents – most strikingly in China and India (Fig. 1), which together account for nearly one-third of the observed total net increase in green leaf area globally (China 25% and India 6.8%, Tables 1 & 3). This greening is seen over 65% of the vegetated lands in the two countries (Supplementary Table 4).

We compare the above results to those from AVHRR data[7], which we have recently updated using the same method as in Zhu et al.[27], for completeness. AVHRR data from the comparable period (2000–2016) show less greening (22% of vegetated lands) and more browning (14%) (Supplementary Table 2). Nearly 60% of the net increase in leaf area is from croplands while forests show a net decrease (Supplementary Table 3). Of the seven MODIS greening clusters (Fig. 1), six are approximately matching in AVHRR data, albeit with less spatial extents and weaker magnitudes, and the sub-Saharan cluster is missing in AVHRR (Supplementary Fig. 1a). The data from the two sensors agree on the magnitude of greening in China and India (Supplementary Table 4), probably because of lower base LAI values (Table 3), (b) larger spatial extents of greening (66 and 69%, respectively; Table 2) and (c) higher relative leaf area changes (18 and 11%, respectively; Table 3). Globally, LAI trends from the two sensors agree over 61% of the vegetated area and the disagreement is mostly in tropical humid areas and Northern high latitudes where AVHRR data quality is poor (Supplementary Fig. 3). The full AVHRR record (1982–2016) shows more greening (41%) and browning (11%) in comparison to the shorter MODIS record, and the patterns exhibit similarities (red circles in Supplementary Fig. 1b) but also important differences (blue circles). The two are not expected to be comparable although both overwhelmingly point to a "Greening Earth"[2–7]. These results are consistent with recent independent estimates of woody and herbaceous cover changes[23].

Human land-use is a dominant driver of Greening Earth.

The above results provide at least four arguments in favor of a greater role for the direct driver than previously thought[2,7,12]. First, cropland greening contributes the most to the net increase in leaf area globally since year 2000 (33%, Table 1). Six of the seven greening clusters (Fig. 1) overlap with the areal pattern of agricultural primary productivity derived independently by Wolf et al.[28] (Supplementary Fig. 2). Cropland greening is mainly

attributable to the direct driver, without discounting the minor but opposing[29,30] contributions of the indirect drivers (CO_2 fertilization has been reported to increase crop production while climate change has been reported to increase or decrease in crop yields depending on location). The green revolution is due to quick-growing hybrid cultivars, multiple cropping, irrigation, fertilizer use, pest control, better quality seeds, farm mechanisation, credit availability, crop insurance programs, etc.[31]. Second, the suggestion that the CO_2 fertilization effect on greening should be seen prominently in hot and arid environments where water limits plant growth[9,20] is not apparent in our analysis. Overall, greening of natural vegetation from these regions (mean annual temperature, MAT, greater than 25 °C and annual total precipitation, 13%, ATP, less than 500 mm, 27%) contributes much less than those from mild (MAT < 25 °C, 87%) and wet (ATP > 500 mm, 73%) climates (Table 1) – this is also true when Table 1 entries are adjusted for vegetated area in each climate class. Third, compared to indirect drivers, gains from cropland production in the northern temperate regions, that incidentally overlap with the greening patterns presented here (Table 1), contribute more toward explaining the increasing amplitude of the seasonal cycle of atmospheric CO_2 concentration[32]. Finally, the large contribution of northern temperate forests to global net greening (16%, Table 1) hints at the importance of large-scale tree plantations in previously low-productive areas of China and silvicultural practices in developed countries, further highlighting the role of the direct driver.

To further appreciate the importance of human land-use management in greening the world, we compare the trends in eleven large countries with sizeable populations and vegetated lands (Table 2). China and India stand out. They are the two most populous countries but rank in the middle in terms of vegetated area. For this reason, and also because they are situated in temperate/sub-tropical climes, they rank either in the middle (China) or towards the bottom (India) in terms of annual-average leaf area (Table 3). Yet they rank at the top (bottom) in terms of proportion of vegetated lands exhibiting greening (browning, Table 2). Consequently, they occupy the top ranks in terms of net increase in leaf area, both on an absolute and relative basis (Table 3). China alone accounts for 25% of the global net increase in leaf area with only 6.6% of global vegetated area. This equals net greening in the three largest countries, Russia, USA and Canada, that together hold 31% of the global vegetated area (Tables 1–3). India is similarly noteworthy. It ranks first (last) in terms of proportion of vegetated area exhibiting greening (browning, Table 2). With only 2.7% of the global vegetated area, India accounts for 6.8% of the global net increase in leaf area, which equals that in USA or Canada, each of which has three times more vegetated area. This statistic is even more remarkable considering that the annual-average leaf area of India is two to three times smaller than that of Canada and USA, respectively (Tables 2 & 3).

The European Union (EU) lands deserve special mention in view of the prominent greening pattern in Fig. 1 (circle 3). This region, like China, ranks in the middle in terms of vegetated land area (Table 2) and average annual leaf area (Table 3) amongst the large countries studied here. Much like China, it ranks at the top (3rd) in terms of vegetated lands exhibiting greening and towards the bottom for browning. These changes produce a top rank for this region for net increase in leaf area (3rd) – 55% of which is due to croplands and 34% to forests (nearly all forests being managed in EU). Recent studies traced the greening in European semi-natural vegetation to land-use practices, principally land abandonment and

afforestation[33–35]. Brazil, on the other hand, ranks towards the bottom because the greening from croplands and pastures is nearly offset by the browning in the forests and cerrado[23]. The dominant cropland contribution to expansive greening in China, India, EU, and USA, highlights the importance of direct driver in global greening.

China and India lead in greening of the Earth.

What explains the large-scale greening of China and India in the 21st century? Forests and croplands contribute 42% and 32%, respectively, to the net increase in leaf area of China while croplands alone contribute 82% in the case of India (forests contribution in India is minor, 4%, and thus was not discussed in detail). Focusing first on forested lands in China, we note an increase (decrease) in tree (non-tree) cover in the greening areas (84% of all forests and other wooded lands) and the opposite in the few (< 1%) browning areas (Fig. 2). Forest inventories reveal a 19% increase in forest area (330×10^3 km^2) in a single decade due in equal measure from expanding natural forests and afforestation (Supplementary Table 5). China is implementing several ambitious programs[36] to conserve and expand forests with the goal of mitigating soil erosion, air pollution and climate change (Supplementary Table 6). Already a third of the 2.08×10^6 km^2 of current forests are plantations (Supplementary Table 5) with rapidly growing young trees less than 40 years old[37]. For example, the mean LAI trend (0.23 m^2 m^{-2} decade^{-1}) for regions with Planted Forest Fraction (PFF) ≥10% is 53% greater than the mean LAI trend (0.15 m^2 m^{-2} decade^{-1}) for regions with PFF < 10%. Similarly, the mean tree cover trend (6.18 % decade^{-1}) for regions with PFF ≥10% is 29% greater than the mean tree cover trend (4.90 % decade^{-1}) for regions with PFF < 10%. Other recent studies attest to the success of said programs in terms of ameliorating land degradation[38], lowering surface temperatures[39] and facilitating carbon sequestration[40], but a strain on water resources has also been noted[41]. All of this emphasizes the significance of human actions in greening the wooded lands of China.

A recent study[42] reported browning trends in natural vegetation of India using MODIS NDVI data, but our re-analysis of the same data does not support this conclusion. That study[42] focused exclusively on the 8 and 4% browning proportions in forests and other woody vegetation classes while ignoring the 19 and 48% greening proportions in these two classes, during the period of their investigation (2001–2014; Supplementary Table 7). The greening proportions increase to 47 and 55% and the browning proportions decline to 1 and 0.5% for the full record (2000–2017). The browning during the shorter period (2001–2014) spans about 42,300 km^2 and is comparable to Chakraborty et al.'s[42] estimate of 55,000 km^2. However, this decreases to 5,000 km^2 during the full period of record (2000–2017). The greening, on the other hand, is 7 times greater (283,300 km^2) during the shorter period and increases to being 80 times greater (401,800 km^2) for the full record. An independent study[43] of trends in MODIS vegetation indices confirms our results.

Turning to cropland greening in China and India, we note that the two had comparable and stable land area under crop cultivation since 2000 (about 1.92 and 2.11×10^6 km^2, Fig. 3). Still, total food production (grains, fruits, vegetables, etc.) has increased significantly (35 to 40%) according to our analysis of data from the Food and Agriculture Organisation[44] (FAO, Supplementary Table 8). For example, total cereal production in China has increased by 43%

from 407×10^6 tonnes in 2000 to 583×10^6 tonnes in 2016. While yields in India are lower, total cereal production increased by 26% during the same period (235 to 295×10^6 tonnes). This is largely due to increasing harvested area through multiple cropping[45] (Fig. 3), which results in the said greening trends. Agricultural intensification in China and India is being facilitated by heavy fertilizer use[46] and surface/ground-water irrigation[47,48] – the two currently rank at the top for the amount of fertilizer use (Supplementary Table 7). Harvested land area at the global scale grew approximately four times faster than the cropland area since 2000 in large part due to these practices in China, India and Brazil[45] and this is reflected in the MODIS greening patterns (Fig. 1). Of particular interest is Brazil's leading and impressive relative changes in agricultural production, fertilizer use and harvested area, however this is due to starting from lower base values (Supplementary Table 8). The observed large-scale greening of China and India is a harbinger of food self-sufficiency for 2.7 billion people in the two top ranked countries in terms of agricultural output (nominal GDP of 1.1 and 0.41 trillion in 2015 US dollars from the agricultural sector in 2015 according to the CIA World Factbook).

Concluding Remarks.

A third of the global vegetated lands are currently greening, i.e. becoming more productive, in a pattern reflective of intensive human use of land for crops and forests across all continents, but most prominently in the two populous countries, China and India. This suggests human land-use management is an important driver of the "Greening Earth"[2–7], accounting for a third, and likely more, of the observed net increase in green leaf area. Therefore, one of the priorities for Earth System Model refinement is a realistic representation of the spatio-temporal dynamics of key land-use practices – multiple cropping, irrigation and fertilizer use, fallowing and abandonment of land, afforestation, reforestation and deforestation. While human exploitation of land will remain a complex dynamic endeavor, monitoring this with space-borne data, especially of the high spatial resolution kind, may offer insights in to how this may be realistically represented in models. Finally, it is important to note that the gain in greenness, which is mostly in the Northern temperate and high latitudes, does not offset the damage from loss of leaf area in tropical natural vegetation (e.g. Brazil, D. R. Congo, Indonesia; Tables 2 & 3) and attendant consequences for ecosystem sustainability and biodiversity.

Methods

MODIS LAI product.

Collection 6 (C6, also Version 6) Terra and Aqua MODIS LAI products (MOD15A2H and MYD15A2H) are used in this study[49,50]. These LAI data sets are provided as 8-day composites in 500 m Sinusoidal projection covering the whole globe. They are further refined by rigorously checking the quality flags of the LAI products and of the simultaneous Vegetation Index products, following the methods described in Samanta et al.[51]. This filtering provides the best quality MODIS LAI observations that minimize any residual contamination from clouds, aerosols, snow, shadow, and etc. The two LAI data sets (i.e. four 8-day composites) are then combined into a 16-day composite by taking the mean of all valid LAI (temporal average). They are then spatially aggregated to generate 0.05° data in a

climate modeling grid (CMG, spatial average). The remaining gaps, though very few, are filled using the climatology of each 16-day composite during 2000–2017. Finally, the annual average LAI for each 0.05° pixel is calculated and used in this study.

The quality of C6 MODIS LAI data sets was comprehensively evaluated against ground-based measurements of LAI and through inter-comparisons with other satellite LAI products[24,25]. These data sets represent the latest and best quality LAI products currently available. They resulted from two decades of research on the LAI algorithm development, testing, refinement and validation – these efforts are described in over 50 peer-refereed journal articles listed at the MODIS Land validation web site[52].

AVHRR LAI3g product.

We generated a new version of the leaf area index data (LAI3gV1) as part of this study based on the methodology described in Zhu et al.[27]. It has global coverage with bi-monthly frequency and is at 1/12° spatial resolution. It spans the period July 1981 to December 2016. It is the longest among current LAI data sets. The full time series of LAI3gV1 data was generated by an artificial neural network (ANN) algorithm that was trained with the overlapping data (2000–2016) of NDVI3gV1 and C6 Terra MODIS LAI product. Here, NDVI3gV1 refers to the new version of the third-generation normalized difference vegetation index data provided by Global Inventory Modeling and Mapping Studies group (GIMMS) Advanced Very High Resolution Radiometer (AVHRR)[53]. The annual average of LAI3gV1 is calculated from 24 observations in each year.

AVHRR LAI data prior to 2000 are not evaluated as required field data are not available. Ground data collected as part of MODIS validation efforts after 2000 were used to test the quality of AVHRR LAI data and these are described in Zhu et al.[27].

MODIS Land Cover Type product.

The land cover (LC) information is provided by the Collection 5.1 MODIS yearly product known as MCD12C1[54]. The spatial resolution of LC is 0.05° in CMG. The International Geosphere-Biosphere Programme (IGBP) classification types provided by MCD12C1 are aggregated into four broad biome types in this study - forests, other woody vegetation (OWV), grasslands, and croplands. Forests include evergreen needleleaf forest, evergreen broadleaf forest, deciduous needleleaf forest, deciduous broadleaf forest, and mixed forest. Other woody vegetation includes closed shrublands, open shrublands, and woody savannas. Grasslands include savannas and grasslands. Croplands include croplands and croplands/natural vegetation mosaic. A static LC map (i.e. the year 2007 map) is used to define the above mentioned four broad biome types.

MODIS Vegetation Continuous Field (VCF) product.

C6 Terra MODIS VCF is a yearly product that presents a continuous, sub-pixel fraction of land surface cover in 250 m Sinusoidal projection from 2000 to 2016[55]. The fraction of land surface cover has three components which are percent tree cover, percent non-tree vegetation cover, and percent non-vegetated cover. The 250 m data are aggregated to 0.05° CMG in this study.

Temperature and precipitation data.

Monthly 0.5° CMG temperature and precipitation data are provided by University of East Anglia Climate Research Unit (CRU) and the latest version is CRU TS4.01[56]. Mean annual temperature (MAT) and annual total precipitation (ATP) were calculated for each year. The climatology of the MAT and ATP is also evaluated during the period of 2000 to 2016. Three climatic zones are defined based on the climatology of MAT: (1) cool, MAT < 10°C, (2) warm, MAT 10–25°C, and (3) hot, MAT > 25°C. Another three climatic zones are defined based on the climatology of ATP: (1) dry, ATP < 500 mm, (2) wet, ATP 500–1000 mm, and (3) humid, ATP > 1000 mm.

Country administrative areas data.

Data on country administrative areas was obtained from the Database of Global Administrative Areas (GADM) hosted by University of California at Davis. The GADM data provide high-resolution shapefiles at all administrative levels, i.e. country level, state/provincial level, etc.[57]. We used the latest version (v2.8) in this study.

FAOSTAT database.

Arable area, harvested area, cereal production and population were obtained from FAOSTAT database hosted by FAO[44]. Crop statistics (i.e. arable area and harvested area) are recorded for 173 types of crops from 1961 to 2015/2016. Arable area and harvested area shown in Fig. 3 are ratios expressed relative to their corresponding values in year 2000. The 2017 population data given by FAO is estimated based on the 2015 Revision of World Population Prospects from the United Nations Population Division.

Forestry inventory data of China.

The forestry inventory data of China is provided by the State Forestry Administration of the People's Republic of China[58]. We used forest statistics documented in the National Continuous Forest Inventory of China (1999–2003 and 2009–2013) to calculate the afforested area, and the changes in forest area and coverage. We also used the planted forest map of China at 1 km spatial resolution, which was obstained from the Seventh National Forest Resource Inventory (2004–2008).

Calculation of LAI trend.

Trends in annual average MODIS LAI (2000 to 2017) and AVHRR LAI3gV1 (1982 to 2016 and 2000 to 2016) are evaluated by the Mann-Kendall test, which is a non-parametric test to detect monotonic trend in time series data. We used the function 'zyp.trend.vector' with Yue-Pilon pre-whitening method provided by R package 'zyp' to conduct the trend test[59]. The trends with $p \leq 0.1$ are considered to be statistically significant in this study. Similar patterns are seen at $p \leq 0.05$ and the seven greening clusters (Fig. 1) are dominantly visible even at $p \leq 0.01$.

Calculation of net leaf area change.

Trends in annual average MODIS LAI were considered as linear when we calculated net leaf area changes during the period 2000 to 2017. The net leaf area changes for a specific region

take in to account the effects from both statistically significant browning and greening areas, and set the areas with statistically insignificant trends to a zero contribution, as shown in Equation (1):

$$\text{Net leaf area changes of a region} = \sum_{i=1}^{N} Tr_i \cdot A_i \cdot Nyr \quad (1)$$

where i represents a pixel with a statistically significant trend, N is the total number of such pixels in the region, Tr_i is the trend of a pixel, Ai is the area of a pixel which varies with latitudes, and Nyr is the length of the study period which is set to 17.

Growing Season Integrated LAI and Annual Average LAI.

Annual average LAI (AA-LAI) is used in our analyses, rather than Growing Season Integrated LAI (GSI-LAI)[7], as it is better suited for a global study such as this that aims to emphasize the importance of land-use management including different cropping cycles (single/multiple) and temporal changes. AA-LAI has the advantage of being simple, can be evaluated for all regions of the globe including those with multiple growing seasons, year-long growing season in the tropical humid forests and when the growing season spans two calendar years. It does not suffer from certain limitations of GSI-LAI, namely, subjective use of thresholds to define the start and end dates of growing season and interpolation of 16-day composite satellite data to daily resolution[6].

Supplementary Material

Refer to Web version on PubMed Central for supplementary material.

Acknowledgements

This work was funded by NASA Earth Science Directorate. R.B.M. acknowledges funding by the Alexander von Humboldt Foundation. T.P. was funded by the NASA Earth and Space Science Fellowship Program. The article processing charges for this publication were paid from funds from NASA Research Grant to Boston University.

References

1. Myneni RB et al. Global products of vegetation leaf area and fraction absorbed PAR from year one of MODIS data. Remote Sens. Environ 83, 214–231 (2002).
2. Myneni RB, Keeling CD, Tucker CJ, Asrar G & Nemani RR Increased plant growth in the northern high latitudes from 1981 to 1991. Nature 386, 698–701 (1997).
3. Zhou L et al. Variations in northern vegetation activity inferred from satellite data of vegetation index during 1981 to 1999. J. Geophys. Res 106, 20069–20083 (2001).
4. Xu L et al. Temperature and vegetation seasonality diminishment over northern lands. Nat. Clim. Change 3, 581–586 (2013).
5. Vickers H et al. Changes in greening in the high Arctic: insights from a 30 year AVHRR max NDVI dataset for Svalbard. Environ. Res. Lett 11, 105004 (2016).
6. Park T et al. Changes in growing season duration and productivity of northern vegetation inferred from long-term remote sensing data. Environ. Res. Lett 11, 084001–12 (2016).
7. Zhu Z et al. Greening of the Earth and its drivers. Nat. Clim. Change 6, 791–795 (2016).
8. Piao S et al. Detection and attribution of vegetation greening trend in China over the last 30 years. Global Change Biol 21, 1601–1609 (2015).

9. Donohue RJ, Roderick ML, McVicar TR & Farquhar GD Impact of CO2 fertilization on maximum foliage cover across the globe's warm, arid environments. Geophys. Res. Lett 40, 3031–3035 (2013).
10. Keenan TF et al. Recent pause in the growth rate of atmospheric CO2 due to enhanced terrestrial carbon uptake. Nat. Commun 7, 13728 (2016). [PubMed: 27922591]
11. Cheng L et al. Recent increases in terrestrial carbon uptake at little cost to the water cycle. Nat. Commun 8, 110 (2017). [PubMed: 28740122]
12. Nemani RR et al. Climate-driven increases in global terrestrial net primary production from 1982 to 1999. Science 300, 1560–1563 (2003). [PubMed: 12791990]
13. Goetz SJ, Bunn AG, Fiske GJ & Houghton RA Satellite-observed photosynthetic trends across boreal North America associated with climate and fire disturbance. Proc. Natl. Acad. Sci. USA 102, 13521–13525 (2005). [PubMed: 16174745]
14. Fensholt R et al. Greenness in semi-arid areas across the globe 1981–2007 — an Earth Observing Satellite based analysis of trends and drivers. Remote Sens. Environ 121, 144–158 (2012).
15. Forkel M et al. Enhanced seasonal CO2 exchange caused by amplified plant productivity in northern ecosystems. Science 351, 696–699 (2016). [PubMed: 26797146]
16. Mao J et al. Human-induced greening of the northern extratropical land surface. Nat. Clim. Change 6, 959–963 (2016).
17. Bjorkman AD et al. Plant functional trait change across a warming tundra biome. Nature 562, 57–62 (2018). [PubMed: 30258229]
18. Prestele R et al. Current challenges of implementing anthropogenic land-use and land-cover change in models contributing to climate change assessments. Earth Syst. Dynam 8, 369–386 (2017).
19. Piao S et al. Lower land-use emissions responsible for increased net land carbon sink during the slow warming period. Nature Geoscience 11, 739–743 (2018).
20. McMurtrie RE et al. Why is plant-growth response to elevated CO2 amplified when water is limiting, but reduced when nitrogen is limiting? A growth-optimisation hypothesis. Funct. Plant Biol 35, 521–14 (2008).
21. Wenzel S, Cox PM, Eyring V & Friedlingstein P Projected land photosynthesis constrained by changes in the seasonal cycle of atmospheric CO2. Nature 538, 499–501 (2016). [PubMed: 27680704]
22. Tian F et al. Evaluating temporal consistency of long-term global NDVI datasets for trend analysis. Remote Sens. Environ 163, 326–340 (2015).
23. Song XP et al. Global land change from 1982 to 2016. Nature 560, 639–643 (2018). [PubMed: 30089903]
24. Yan K et al. Evaluation of MODIS LAI/FPAR product Collection 6. Part 1: consistency and improvements. Remote Sensing 8, 359–16 (2016).
25. Yan K et al. Evaluation of MODIS LAI/FPAR product Collection 6. Part 2: validation and intercomparison. Remote Sensing 8, 460–26 (2016).
26. Knyazikhin Y, Martonchik JV, Myneni RB, Diner DJ & Running SW Synergistic algorithm for estimating vegetation canopy leaf area index and fraction of absorbed photosynthetically active radiation from MODIS and MISR data. J. Geophys. Res 103, 32257–32275 (1998).
27. Zhu Z et al. Global data sets of vegetation leaf area index (LAI)3g and fraction of photosynthetically active radiation (FPAR)3g derived from global inventory modeling and mapping studies (GIMMS) normalized difference vegetation index (NDVI3g) for the period 1981 to 2011. Remote Sensing 5, 927–948 (2013).
28. Wolf J et al. Biogenic carbon fluxes from global agricultural production and consumption. Global Biogeochem Cy 29, 1617–1639 (2015).
29. Lobell DB, Schlenker W & Costa-Roberts J Climate trends and global crop production since 1980. Science 333, 616–620 (2011). [PubMed: 21551030]
30. Rosenzweig C & Parry ML Potential impact of climate change on world food supply. Nature 367, 133–138 (1994).
31. Jain HK Green Revolution: History, Impact and Future (Studium Press LLC, Houston, 2010).

32. Zeng N et al. Agricultural Green Revolution as a driver of increasing atmospheric CO2 seasonal amplitude. Nature 515, 394–397 (2014). [PubMed: 25409829]
33. Buitenwerf R, Sandel B, Normand S, Mimet A & Svenning JC Land surface greening suggests vigorous woody regrowth throughout European semi-natural vegetation. Global Change Biol 27, 792–13 (2018).
34. Fuchs R, Herold M, Verburg PH, Clevers JGPW & Eberle J Gross changes in reconstructions of historic land cover/use for Europe between 1900 and 2010. Global Change Biol 21, 299–313 (2014).
35. Fuchs R et al. Assessing the influence of historic net and gross land changes on the carbon fluxes of Europe. Global Change Biol 22, 2526–2539 (2016).
36. Zhang Y et al. Multiple afforestation programs accelerate the greenness in the 'Three North' region of China from 1982 to 2013. Ecol. Indic 61, 404–412 (2016).
37. Zhang Y, Yao Y, Wang X, Liu Y & Piao S Mapping spatial distribution of forest age in China. Earth and Space Science 4, 108–116 (2017).
38. Tong X et al. Increased vegetation growth and carbon stock in China karst via ecological engineering. Nat Sustain 1, 44–50 (2018).
39. Peng SS et al. Afforestation in China cools local land surface temperature. Proc. Natl. Acad. Sci. USA 111, 2915–2919 (2014). [PubMed: 24516135]
40. Lu F et al. Effects of national ecological restoration projects on carbon sequestration in China from 2001 to 2010. Proc. Natl. Acad. Sci. USA 115, 4039–4044 (2018). [PubMed: 29666317]
41. Feng X et al. Revegetation in China's Loess Plateau is approaching sustainable water resource limits. Nat. Clim. Change 6, 1019–1022 (2016).
42. Chakraborty A, Seshasai MVR, Reddy CS & Dadhwal VK Persistent negative changes in seasonal greenness over different forest types of India using MODIS time series NDVI data (2001–2014). Ecol. Indic 85, 887–903 (2018).
43. Zhang Y, Song C, Band LE, Sun G & Li J Reanalysis of global terrestrial vegetation trends from MODIS products: Browning or greening? Remote Sens. Environ 191, 145–155 (2017).
44. Food and Agriculture Organization of the United Nations. FAOSTAT database http://www.fao.org/faostat/ (2018).
45. Ray DK & Foley JA Increasing global crop harvest frequency: recent trends and future directions. Environ. Res. Lett 8, 044041–11 (2013).
46. Lu C & Tian H, Global nitrogen and phosphorus fertilizer use for agriculture production in the past half century: shifted hot spots and nutrient imbalance. Earth Syst. Sci. Data, 9, 181–192 (2017).
47. Mueller ND et al. Closing yield gaps through nutrient and water management. Nature 490, 254–257 (2012). [PubMed: 22932270]
48. Ambika AK, Wardlow B & Mishra V Remotely sensed high resolution irrigated area mapping in India for 2000 to 2015. Sci. Data 3, 160118–14 (2016). [PubMed: 27996974]
49. Myneni R, Knyazikhin Y & Park T MOD15A2H MODIS/Terra leaf area index/FPAR 8-day L4 global 500m SIN grid V006 data set 10.5067/MODIS/MOD15A2H.006 (2015).
50. Myneni R, Knyazikhin Y & Park T MYD15A2H MODIS/Aqua leaf area index/FPAR 8-day L4 global 500m SIN grid V006 data set 10.5067/MODIS/MYD15A2H.006 (2015).
51. Samanta A et al. Comment on 'Drought-induced reduction in global terrestrial net primary production from 2000 through 2009'. Science 333, 1093–1093 (2011).
52. MODIS land team. Validation: status for LAI/FPAR (MOD15) https://landval.gsfc.nasa.gov/ProductStatus.php?ProductID=MOD15 (2018).
53. Pinzon J & Tucker C A non-stationary 1981–2012 AVHRR NDVI3g time series. Remote Sensing 6, 6929–6960 (2014).
54. Friedl MA, McIver DK, Hodges J & Zhang XY Global land cover mapping from MODIS: algorithms and early results. Remote Sens. Environ 83, 287–302 (2002).
55. Dimiceli C et al. MOD44B MODIS/Terra vegetation continuous fields yearly L3 global 250m SIN grid V006 data set 10.5067/MODIS/MOD44B.006 (2015).

56. Harris IC & Jones PD CRU TS4.01: Climatic Research Unit (CRU) Time-Series (TS) version 4.01 of high-resolution gridded data of month-by-month variation in climate (Jan. 1901-Dec. 2016) http://doi.org/10/gcmcz3 (2017).

57. Center for Spatial Sciences at the University of California at Davis. The Database of Global Administrative Areas (GADM) maps and data https://gadm.org/ (2018).

58. State Forestry Administration of the People's Republic of China. China forestry database: national continuous forest inventory of China (In Chinese) http://data.forestry.gov.cn/lysjk/ (2018).

59. Bronaugh D & Werner A Package 'zyp'. CRAN Repository (2013).

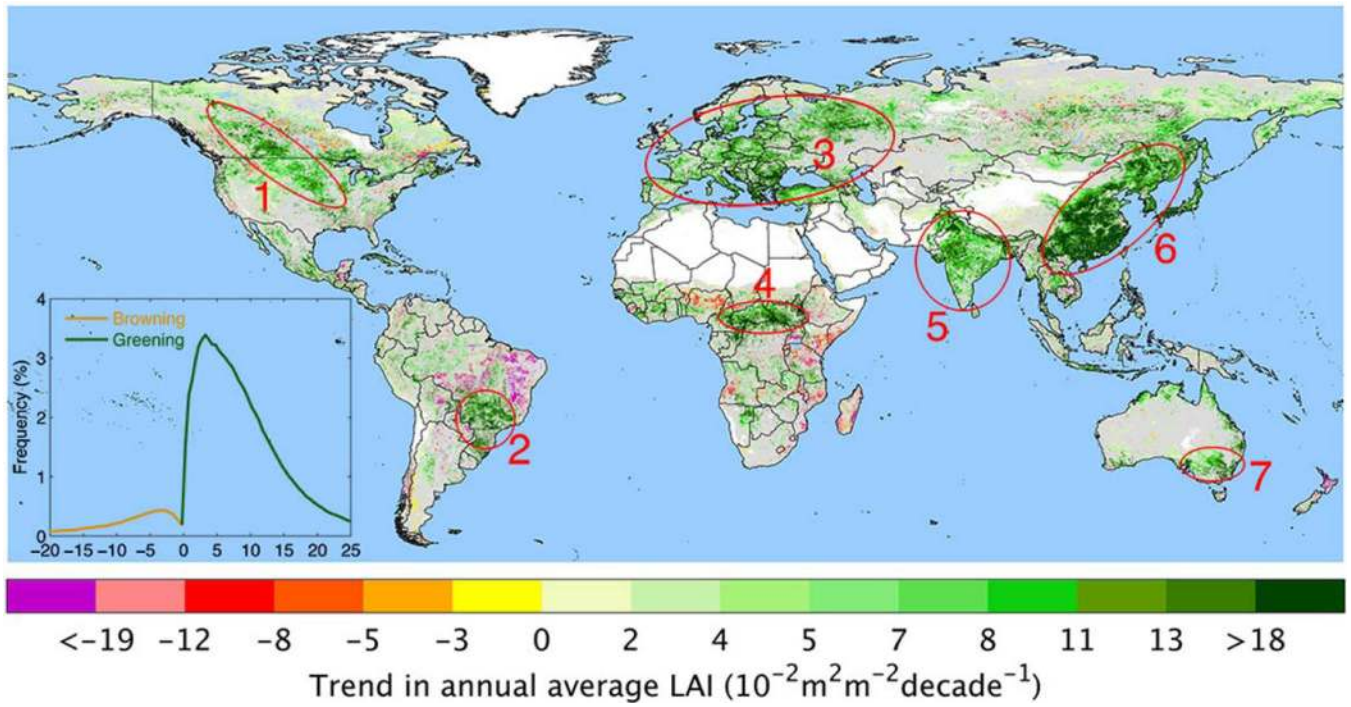

Fig. 1|. Map of trends in annual average MODIS LAI over 2000–2017.

Statistically significant trends (Mann-Kendall test, $p \leq 0.1$) are color coded. Grey areas show vegetated land with statistically insignificant trends. White areas depict barren lands, permanent ice-covered areas, permanent wetlands and built-up areas. Blue areas represent water. The inset shows the frequency distribution of statistically significant trends. The highlighted greening areas in red circles overlap with croplands mostly with the exception of circle number 4. Similar patterns are seen at $p \leq 0.05$ and the seven greening clusters are dominantly visible even at $p \leq 0.01$.

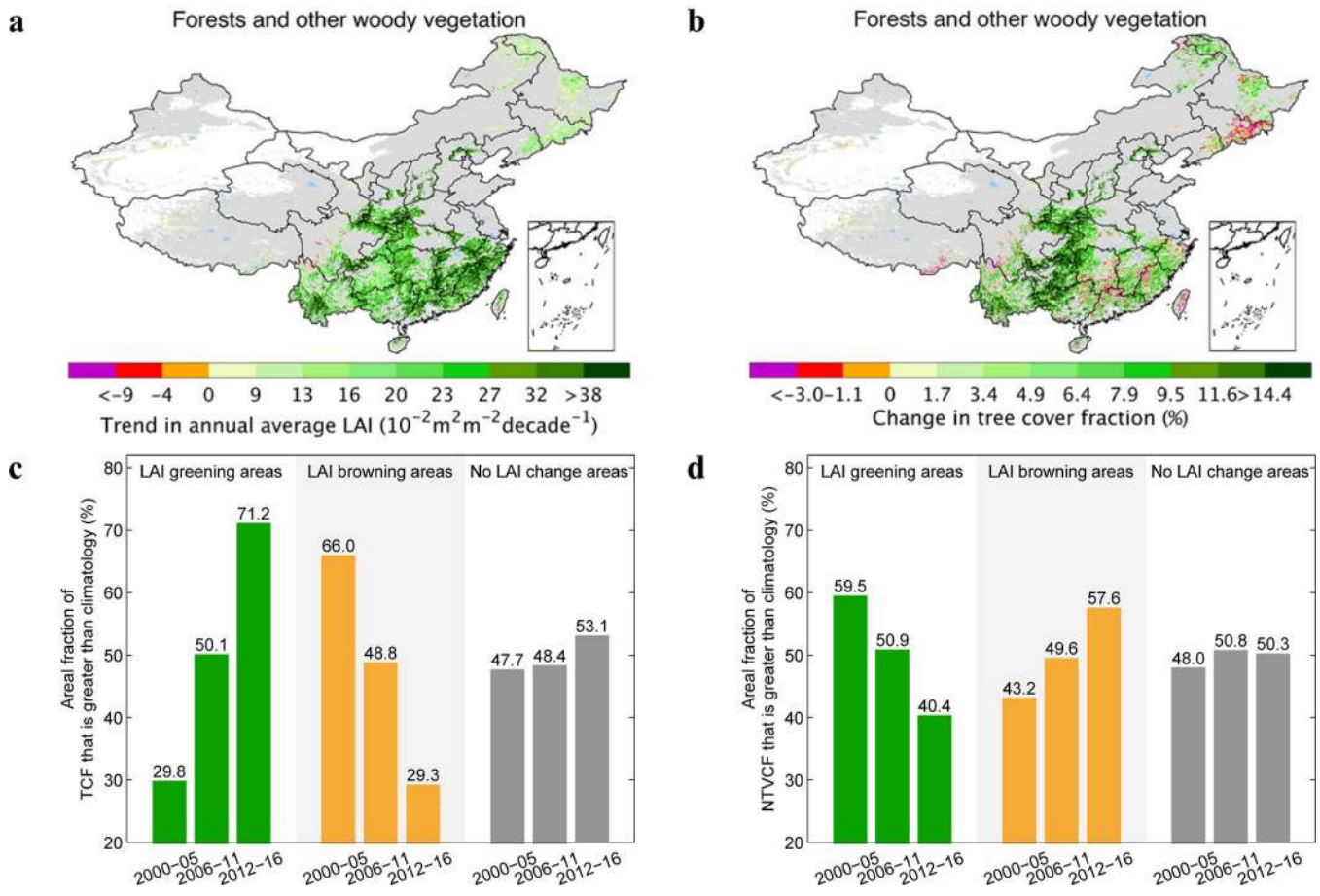

Fig. 2|. Trends in forests and other woody vegetation of China.

a, Trend in annual average LAI. **b**, Change in tree cover fraction between 2014–16 and 2000–02 over areas showing statistically significant LAI trends in (**a**). Grey areas show vegetated land with statistically insignificant LAI trends or predominantly herbaceous vegetation. White areas depict land that is not vegetated. Black lines are boundaries of the first-level administrative divisions. **c**, **d**, Areal fraction of tree cover fraction (TCF) (**c**) and non-tree vegetation cover fraction (NTVCF) (**d**) over forests and other woody vegetation that is greater than the climatology during a particular period, i.e. 2000–05, 2006–11, and 2012–16. Climatology is the mean of values from long-term observations. The colors further confine the analysis to LAI greening (green bars), browning (browning bars) and no LAI change (grey bars) areas.

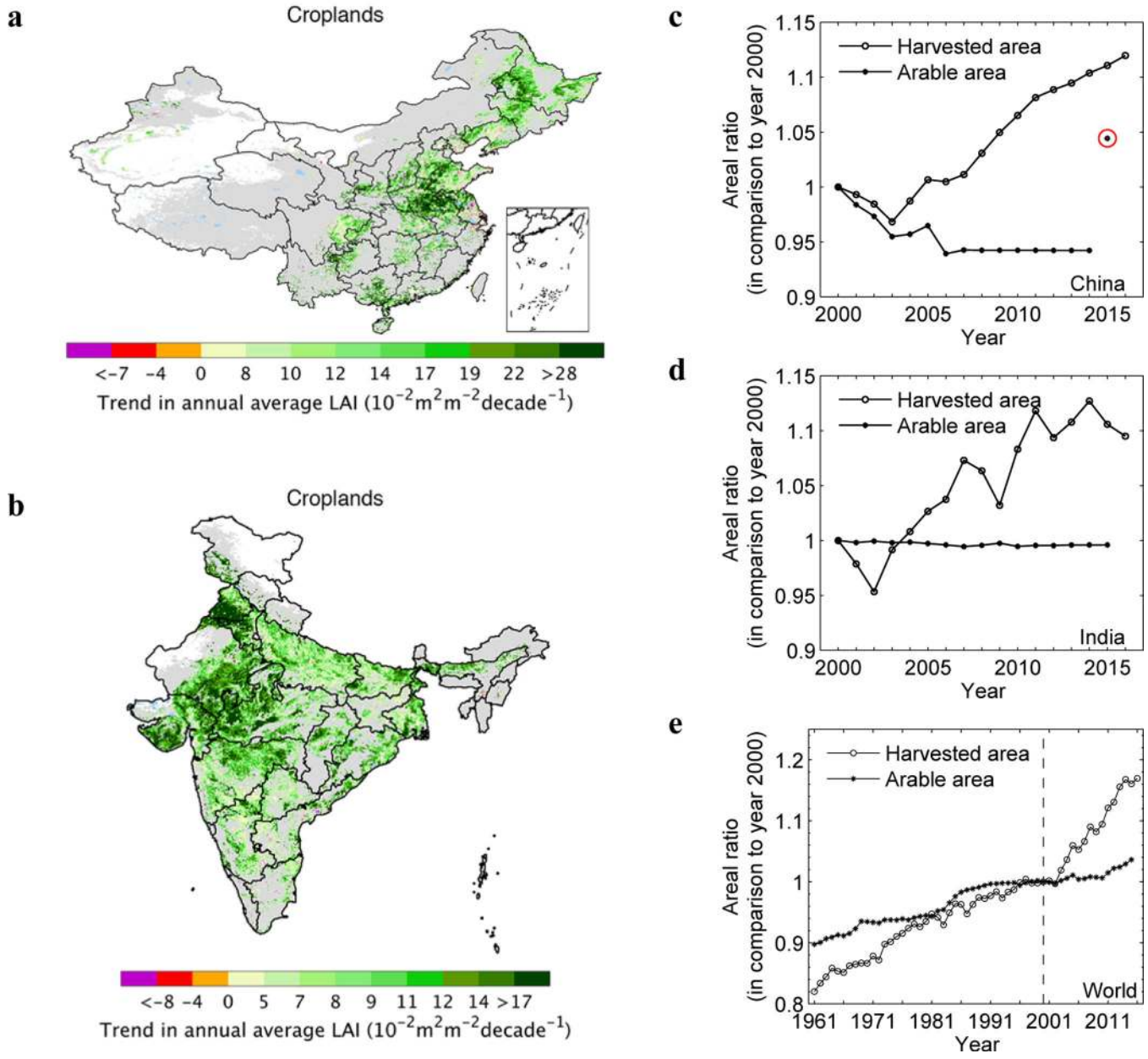

Fig. 3|. Leaf area trends in croplands of China and India.

a, **b**, Trend in annual average LAI over croplands in China (**a**) and India (**b**). **c–d**, Ratio of harvested area (circle) and arable area (asterisk) with respect to year 2000 values for China (**c**), India (**d**) and the world (**e**). The asterisk circled in red in (**c**) is an outlier. The vertical dash line in (**e**) indicates the year 2000.

Table 1|

Net changes in leaf area (10^{-1} million km^2) over the period 2000–2017, i.e. the difference between greening and browning.

	Forests	Other woody vegetation	Grasslands	Croplands	All vegetation
Global	16.72	11.50	7.85	17.85	53.91
		By latitude			
>50° S/N	4.78	3.48	0.80	2.36	11.41
25° S/N–50° S/N	8.87	3.38	4.61	10.76	27.62
25° S–25° N	3.08	4.64	2.44	4.73	14.88
		By mean annual temperature (MAT)			
MAT < 10 °C	7.48	3.61	4.04	5.23	20.36
MAT 10–25 °C	7.92	5.82	2.46	7.70	23.89
MAT > 25 °C	1.32	2.06	1.35	4.92	9.65
		By annual total precipitation (ATP)			
ATP < 500 mm	1.76	4.08	3.86	2.66	12.35
ATP 500–1000 mm	7.37	2.29	1.30	9.23	20.20
ATP > 1000 mm	7.59	5.13	2.69	5.95	21.35

Table 2|

Ranking of eleven largest countries by vegetated land area and proportion of vegetated lands showing statistically significant trends.

Rank	Vegetated land area (million km^2)	Proportion of vegetated lands showing greening (%)	Proportion of vegetated lands showing browning (%)
1	Russia (16.04)	India (69.0)	Brazil (11.6)
2	USA (8.91)	China (65.6)	Indonesia (6.8)
3	Canada (8.47)	EU* (51.4)	Argentina (6.7)
4	Brazil (8.31)	Canada (41.6)	Canada (5.7)
5	Australia (7.50)	Russia (38.0)	D. R. Congo (4.5)
6	China (7.19)	USA (33.3)	USA (2.9)
7	EU* (4.22)	Mexico (28.4)	Russia (2.7)
8	India (2.94)	Brazil (25.6)	Mexico (2.4)
9	Argentina (2.57)	Australia (24.4)	China (1.3)
10	D. R. Congo (2.28)	D. R. Congo (23.7)	EU* (1.3)
11	Mexico (1.88)	Indonesia (19.7)	Australia (0.8)
12	Indonesia (1.80)	Argentina (13.2)	India (0.8)

The following large countries were excluded because of unfavorable climatic conditions for vegetation growth: Algeria, Kingdom of Denmark that includes Greenland, Kazakhstan and Saudi Arabia. European Union is included here, although it is not a country.

Table 3|

Ranking of eleven largest countries by leaf area and its change during 2000–2017.

Rank	Annual average leaf area in 2000 (million km^2)	Net change in leaf area (10^{-1} million km^2)	Net change in leaf area (%)
1	Brazil (29.68)	China (13.51)	China (17.80)
2	Russia (12.36)	Russia (7.57)	India (11.10)
3	USA (8.93)	EU* (4.02)	EU* (7.78)
4	Indonesia (8.69)	India (3.65)	Canada (7.13)
5	D. R. Congo (8.50)	USA (3.59)	Russia (6.62)
6	China (7.64)	Canada (3.35)	Australia (5.62)
7	Canada (5.41)	Australia (2.83)	USA (4.55)
8	EU* (5.23)	Brazil (1.12)	Mexico (4.07)
9	Australia (5.19)	Mexico (0.96)	Argentina (1.70)
10	India (3.33)	D. R. Congo (0.96)	Brazil (1.54)
11	Mexico (2.66)	Indonesia (0.51)	D. R. Congo (1.34)
12	Argentina (2.16)	Argentina (0.13)	Indonesia (0.83)

The following large countries were excluded because of unfavorable climatic conditions for vegetation growth: Algeria, Kingdom of Denmark that includes Greenland, Kazakhstan and Saudi Arabia. European Union is included here, although it is not a country.